University of Rhode Island
DigitalCommons@URI

Open Access Master's Theses

2013

Development of a Self-Tuning Amplifier for Piezoelectric Transducer Evaluations

Hayden N. Radke
University of Rhode Island, hradke@gmail.com

Follow this and additional works at: https://digitalcommons.uri.edu/theses

Terms of Use
All rights reserved under copyright.

Recommended Citation
Radke, Hayden N., "Development of a Self-Tuning Amplifier for Piezoelectric Transducer Evaluations" (2013). *Open Access Master's Theses.* Paper 80.
https://digitalcommons.uri.edu/theses/80

This Thesis is brought to you by the University of Rhode Island. It has been accepted for inclusion in Open Access Master's Theses by an authorized administrator of DigitalCommons@URI. For more information, please contact digitalcommons-group@uri.edu. For permission to reuse copyrighted content, contact the author directly.

DEVELOPMENT OF A SELF-TUNING AMPLIFIER FOR PIEZOELECTRIC TRANSDUCER EVALUATION

BY

HAYDEN RADKE

A THESIS SUBMITTED IN PARTIAL FULFILLMENT OF THE

REQUIREMENTS FOR THE DEGREE OF

MASTERS OF SCIENCE

IN

OCEAN ENGINEERING

UNIVERSITY OF RHODE ISLAND

2013

MASTER OF SCIENCE THESIS

OF

HAYDEN RADKE

APPROVED:

Thesis Committee:

Major Professor Harold Vincent

James Hu

Peter Swaszek

Nasser H. Zawia

DEAN OF THE GRADUATE SCHOOL

UNIVERSITY OF RHODE ISLAND

2013

ABSTRACT

This thesis presents an automated method of tuning underwater transducers. Typically, the efficiency of a piezoelectric transducer's output power is limited by an electrical mismatch between the voltage source and transducer. This mismatch is due to the capacitive reactance of the piezoelectric element. The addition of an appropriately sized inductor to the system can effectively cancel the capacitive reactance and introduce an "electrical resonance" at a given frequency. A prototype system is described and constructed which leverages the effects of additional inductance to produce significant gains in output power of a transducer. This Automated Tuning System (ATS) consists of switching inductor network controlled by a tuning algorithm. Testing demonstrates that the ATS is capable of producing significant off-band gains in transduction efficiency as well as considerably extending the functional bandwidth of the transducer.

CONTENTS

LIST OF TABLES

LIST OF FIGURES

CHAPTER 1

INTRODUCTION

A typical implementation of a piezoelectric acoustic source consists of the following: a signal source, amplifier, cable, and a piezoelectric element. In order to maximize the efficiency of this system the output impedance of the amplifier must be matched to the combined electro-mechanical impedance of the cable and transducer. Because the electrical characteristics of each transducer and cable combination are unique, optimizing the system is a time consuming process; one which is often neglected in favor of increased input power. From an academic standpoint the majority of the literature pertaining to the electrical tuning of piezo-elements is dominated by high frequency (>1MHz) applications leaving room for speculation about the benefits of variable tuning within the range of transducers typically employed in marine applications (5-200kHz).

Manufacturers generally consider impedance matching a one time engineering cost while developing a complete system. In the lab however, a single amplifier is often employed to drive a plethora of unique piezoelectric elements making the process of tuning much more frequent and tedious. One intention of this project is to produce a system which will automatically match the amplifier to a variety of piezoelectric elements thus streamlining the process considerably. Commercially there may be some value in a "universal" amplifier for a range of transducers, but this is not the aim of this study. Instead, the focus of the project is to develop a tool to simplify the test and evaluation of prototype piezoelectric projectors within

a laboratory setting. The process of impedance matching the amplifier to the transducer generally produces some useful measurements. One such measurement is the magnitude and phase of the transducer impedance vs frequency. This is often one of the first measurements made upon a prototype transducer, because the impedance vs frequency gives an indication of the resonance and bandwidth of a transducer.

The objectives of this project are as follows: First, the process of basic transducer evaluation is to be automated and a prototype transducer tuning network constructed. Second, a tuning algorithm will be developed and compared against an analytic solution. Finally, the performance of a standard (un-tuned) and tuned transducer system will be explored. It is expected that the completed system will not only streamline laboratory testing, but also extend the functional bandwidth and power output of a range of piezoelectric transducers.

CHAPTER 2

BACKGROUND

2.1 Basic Transducer Analysis

The Van Dyke equivalent circuit (Figure 2.1) is a commonly employed representation of an an electric field transducer. The Electrical components of the equivalent circuit represent both the electrical and mechanical properties of a piezoelectric element. The electrical dissipation factor (R_o), and clamped capacitance(C_0), represent the electrical characteristics of the transducer. The electrical equivalent capacitance, inductance, and resistance (C_e, L_e, R_e) describe the electrical effects of the mechanical motion of the transducer (as such they are also referred to as "motional" components). The equivalent circuit can be extended to support multiple resonant modes with additional parallel RLC motional elements.

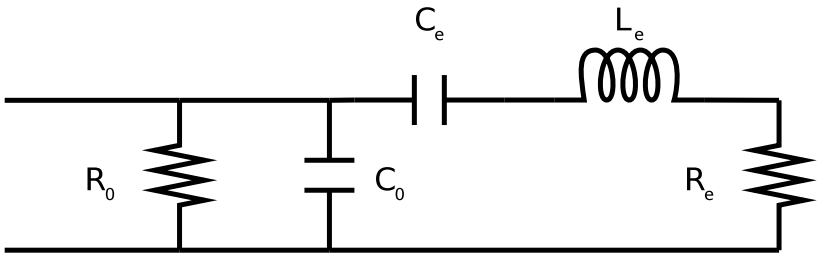

Figure 2.1: Van Dyke Equivalent Circuit

The values of the circuit components can be derived from the physical parameters of the piezoelectric element (mass, mechanical resistance, stiffness, etc). They can also be determined experimentally from impedance measurements. The experimental approach requires minimal prior knowledge of the transducer element

and directly computes the impedance (and inversely the admittance) of the system. For the purpose of this paper the transducer characteristics will generally be related back to impedance measurements. The admittance (Y) is the reciprocal of the electrical impedance (Z) of a transducer. Experimentally, we can measure the admittance $Y = G + jB$ where G is the conductance and B is the susceptance. As the complex ratio of current over voltage the admittance can be used to describe the electrical efficiency of a driven transducer. Mathematically, we can describe the input admittance of the Van Dyke circuit as[3]:

$$Y = G_0 + j\omega C_0 + 1/(R_e + j\omega L_e + 1/j\omega C_e) \tag{2.1}$$

where $G_0 = 1/R_0$. At the mechanical resonance of this system the magnitude of the admittance reaches a maximum ($|Y|_{MAX}$). This occurs when the reactance of the motional components cancel ($\omega L_e = 1/\omega C_e$). Thus, at mechanical resonance the Van Dyke equivalent circuit becomes Figure 2.2.

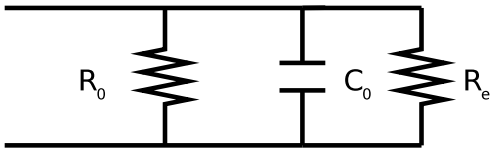

Figure 2.2: Equivalent circuit at mechanical resonance.

The equivalent circuit illustrated in Figure 2.2 is a common simplification of the Van Dyke Circuit and is generally employed to describe a transducers characteristics at resonance. The admittance of a transducer at resonance can now be described as:

$$Y = G_0 + j\omega C_0 + 1/R_e \tag{2.2}$$

We can also describe the flow of energy into a transducer with the power factor (P_f) and quality factor (Q_e electrical, Q_m mechanical). The power factor is a relation of the phase angle ($\phi = tan^{-1}(B/G)$) between the driving voltage and current,

$P_f = cos\phi = W/VI$, where W is absorbed power and the magnitude of the voltage and current are V and I respectively. By inspection we can see that the power factor reaches unity when the driving voltage and current are in phase. Furthermore the power factor at unity represents a case where all of the driving current is dissipated within the transducer. Lastly, we can see that $P_f = 1$ when $B/G = 0$. The quality factor (Q) of a transducer has a plethora of mathematical definitions, most simply, the Q can be defined as a ratio of stored energy to dissipated energy. Define α as the time it takes oscillatory energy to decay to $1/e$ of its peak value, WT as the energy within the element per cycle, and T as time[2, 3]:

$$Q = 2\pi \frac{\text{(energy stored per cycle)}}{\text{(energy dissipated per cycle)}} = 2\pi \frac{WT}{\alpha WT} \tag{2.3}$$

Thus the electrical quality factor (Q_e) is a ratio of the susceptance to conductance (B/G). In other words the Q_e serves as a measure of the power factor. From the preceding discussion a large P_f would require a small Q_e. The mechanical quality factor (Q_m) serves as a measure of the "sharpness" of the power curve making it a measure of both sensitivity and bandwidth of the transducer. Given a transducer with a single resonant frequency ω_r, with half power points ($W_{MAX}/2$) located at ω_1 & ω_2 the $Q_m$can be defined as:

$$Q_m = \omega_r/(\omega_2 - \omega_1) \tag{2.4}$$

Thus a low Q_m is equivalent to a broadband transducer. A feature that is generally desirable in underwater applications.

Because of the large difference between the acoustic impedance in air and water measurements of the Q_m of a transducer in air and water differ greatly. A high Q_m in air points to low internal losses and thus a high efficiency. However, the same transducer measured in water might also have a low Q_m. This not only illustrates

the importance of correctly characterizing a transducer but also to the trade off between high sensitivity and bandwidth.

2.2 Fundamentals of Tuning

The goal of electrically tuning or "impedance matching" a transducer is to make the transfer of energy between a power source and transducer as efficient as possible. Fundamentally, this can be done with the addition of a transformer or inductor to the system. A well accepted means of impedance matching is the introduction of a transformer between the amplifier and transducer. We can define a transformer by the number of turns on the primary (N_P) and secondary (N_s) windings, where the transformer ratio $N = N_s/N_p$. The behavior of an ideal transformer is described as[8]:

$$V_s = NV_p;\ I_s = I_p/N;\ Z_P = Z_L/N^2 \tag{2.5}$$

Not only is the voltage multiplied by the transformer ratio but the load impedance is transformed by the square of the turns ratio. For example, an amplifier with an output impedance of 50Ω can be matched to a transducer with an impedance of $5k\Omega$ with a turns ratio of 10. Inherently, the transformers construction also adds some amount of parallel inductance to the system. Revisiting the Van Dyke equivalent circuit of a transducer at resonance (Figure 2.2) we see that at resonance the reactance of the transducer is now represented entirely by the clamped capacitance (C_0). Theoretically, by introducing an inductor into the system the reactive portion of C_0 could be canceled, further increasing the power factor of the system. As the reactance of a transducer is a function of frequency the addition of a fixed inductor offers benefits at the tuned frequency, for simplicity the case of inductive tuning at resonance is described.

The introduction of a parallel tuning inductor positively effects the Receive Voltage Sensitivity (RVS) yet shows no effect on the Transmitting Voltage Re-

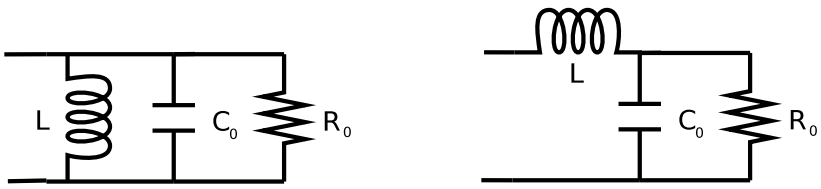

Figure 2.3: Parallel and Series (left and right respectively) inductive tuning equivalent circuits.

sponse (TVR) [2, 3]. An inductor placed in series has the opposite effect, increasing TVR while not effecting the RVS. Under the tuned condition the capacitive and inductive reactance must cancel, thus the source impedance must equal the complex conjugate of the load to achieve maximum power transfer, XC = XL*. The reactance of C_0 can be described as $1/\omega C_0$, the introduction of a parallel tuning inductor ($L_P = 1/\omega_r^2 C_0$) effectively cancels the transducer's reactance at resonance. In other words the correct value of L_P the reactance of Figure 2.3 becomes zero at the resonant frequency. The Q of this parallel system can now be described by $Q = R/X_L$[1]. The parallel inductance does not effect a voltage applied to the transducer and thus has no effect on the transmit response. The series tuning case lowers the transducers input impedance requiring less voltage to drive. Equations 2.6&2.7 relate the Q_e of the series tuned circuit depicted in Figure 2.3 to the value of the series inductor[3]. This relation shows that the Q_e becomes very large as the value of $L_s$approaches that of $L_P$ie $1/\omega_r^2 C_0$ pointing to a limiting inductance value which does not increase output power.

$$Q_e = \frac{\omega_r C_0 R_0 R_e}{R_0 + R_e} \tag{2.6}$$

$$L_s = \frac{(1/\omega_r^2 C_0) Q_e^2}{1 + Q_e^2} \quad \begin{cases} L_s \Rightarrow L_p & Q_e \gg 1 \\ L_s \Rightarrow Q_e^2 L_p & Q_e \ll 1 \end{cases} \tag{2.7}$$

[2, 3] describe the series and parallel tuned RVS and TVR of a transducer

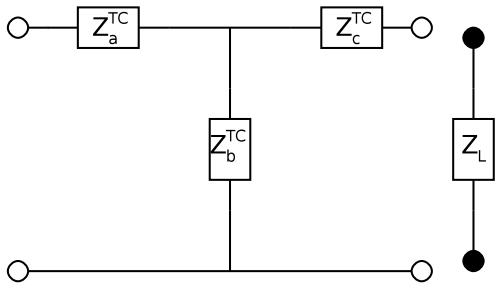

Figure 2.4: Lumped impedance model of tuning circuit and transducer.

and note that both take the shape of a bandpass filter. The transducers voltage response is reduced at a rate of 6dB per octave beyond the resonant region [3]. The magnitude and bandwidth of this "filter" depends on the Q_e of the system and Q_m of the transducer. The addition of a tuning inductor has the potential to significantly narrow the bandwidth of the system, because of this tuning inductors are rarely employed in broad band applications.

Another method of representing a tuning network and transducer is through an equivalent circuit of lumped impedances [8]. Figure 2.4 shows the layout of a T network with the load and tuning circuit input impedances marked. The lumped impedances of an existing network can be measured by taking a series of open circuit and closed circuit impedance measurements across the network's input and output. The effective impedance of the tuning network and transducer can now be described using:

$$Z_{Total} = Z_a^{TC} + \frac{Z_b^{TC}(Z_c^{TC} + Z_L^{TC})}{Z_b^{TC} + Z_c^{TC} + Z_L^{TC}} \tag{2.8}$$

Continuing to employ stacked T networks, [8] extended this method to include the effects of cable electrical characteristics.

Developing an equivalent circuit becomes more time consuming for transducers with multiple resonances [8] or when array interactions must be considered. A potential solution to this problem is to determine the tuning inductance experimen-

tally rather than analytically. An impedance matching circuit that contained both a variable inductor and transformer could accommodate a range of frequencies, impedances, and transducer elements as well as allow "experimental tuning."

In an effort to extend the functionality of the amplifier circuitry as well as minimize the labor required to tune a piezoelectric element the idea of an automated tuning network was proposed. Previously work by Polk in 1978 at MIT [7]outlined a scheme to increase the acoustic power radiated from ultrasonic piezoelectric ceramics using a variable tuning circuit in his laboratory. Now, using current technology, the plan is to develop an automated circuit which provides tuning capability to existing amplifier circuitry. The literature is somewhat sparse in regards to the details of the effects of tuning circuits on transducers used in the frequency range of typical underwater applications. Electrical tuning is common practice at high frequencies especially in Nondestructive Evaluation (NDE) applications.

Ramos [9] achieved nearly a 100% increase in bandwidth and sensitivity in Emitter Receiver (E/R) applications by using a pair of tuned shunt circuits with a piezo-element resonant near 1MHz. Each tuning circuit was designed to match the complex impedance of the element to the amplifier and data acquisition unit (DAQ). By rapidly switching between the emitter and receiver tuning circuits Ramos was able to optimize both the transmit and receive roles of a single element producing significant gains over a common tuning network.

Xu [12] produced an variable electrical tuning network consisting of a fixed inductor with a variable capacitor. Although the focus of Xu's work was in piezoelectric oscillators (400Mhz), fundamentally the technique employed to shift the driven resonance of a piezoelectric element remains the same. Xu was able to electrically tune the resonant peak of his system across a range of 34% by varying the capacitance of the driving circuit.

Snook [10] offered a comparison of various piezoelectric materials commonly used in NDE systems. Snook noted the importance of impedance matching the transducer to the amplifier and DAQ during transducer comparisons. Snook observed a significant shift in resonance characteristics between tuned and un-tuned elements. Again Snook's study was on HF (20-150MHz) systems. Undoubtedly, the benefits of electrically tuning piezoelectric transducers can be significant, and theoretically the benefits seen at ultrasonic frequencies should be exploitable within the audio band as well.

This project aims to streamline the process of performing the baseline evaluation of transducers in the laboratory. More significantly, it aims to fill a knowledge gap pertaining to the potential benefits of electrical tuning on audio band transducers.

The aforementioned articles serve to add two key goals to the project: First, achieve significant gains in radiated acoustic power by employing electrical tunning. Second, replicate the 20-30% resonant frequency shift seen in HF applications [10, 12, 6] at significantly lower frequencies. If these goals can be met, this research has the potential to branch into further investigation of the applicability of variable electrical tuning beyond the laboratory.

CHAPTER 3

METHODS

The experiment might best be thought of as containing three parts. First, it seems prudent to experimentally verify that electrical tuning at audio frequencies is worthwhile. Next a variable tuning system must be designed and constructed. Finally, the Automated Tuning System (ATS) can be programed and tested.

3.1 Experimental Evaluation of Tuning Theory

In an effort to verify that the addition of series inductance can produce measurable (perhaps significant) effects on the transmitting response of a underwater transducer the following experiments were performed. First, generic underwater transducer evaluation was performed, from these measurements the Van Dyke equivalent parameters can be derived. Then the desired series tuning inductance could be calculated. Finally the series tuned system could be evaluated.

Surprisingly the first measurements made upon an underwater transducer are typically performed in air. Because the acoustic impedance of air is much smaller than that of water the transducer can be considered to be "free" or unloaded. Often the first step of transducer evaluation is to produce a plot of the complex impedance. By measuring the voltage across a resistor of known value (R>>Z) in series with the transducer (in air) the admittance can be solved by:

$$Y = \frac{1}{Z} \approx \frac{V_R}{V_0 R} \tag{3.1}$$

$$V_R = V_0 - V_X \tag{3.2}$$

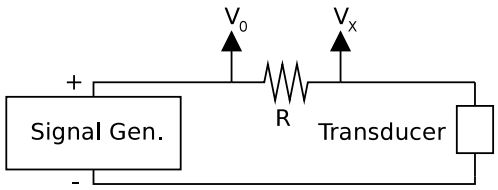

Figure 3.1: Impedance measurement setup.

The test circuit (Figure 3.1) is then swept by a constant voltage source over the frequency range of interest. The Frequency dependence of the voltage values are then computed with a Fast Fourier Transform (FFT) and the frequency based admittance curve is produced using equation 3.1 (See Appendix A for code). The next step involves measuring the free capacitance (C_f) using an LCR meter at a low frequency. Combining the results of these two measurement sources the following system parameters can be computed (k_{eff} is the electromechanical coupling factor) :

$$k_{eff}^2 = 1 - (f_r - f_a)^2 \tag{3.3}$$

$$C_0 = C_f(1 - k_{eff}^2) \tag{3.4}$$

$$C_e = k_{eff}^2 C_f \tag{3.5}$$

Finally, the equivalent electrical inductance and the mechanical quality factor can be derived:

$$L_e = \frac{1}{\omega_r^2 C_e} \tag{3.6}$$

$$\frac{1}{R_e} \approx |Y|_{max} \Rightarrow Q_m = \omega_r L_e R_e \approx \omega_r L_e |Y|_{max} \quad \text{for} \quad Q_e > 30 \tag{3.7}$$

At this point, all of the parameters of the Van Dyke equivalent circuit (Figure 2.1) have been represented using measured values and the transducer can be mathematically represented using the equations outlined in the Background section.

For an investigation into the effects of tuning an International Transducer Corporation (ITC) 3013 underwater transducer was chosen from the URI Ocean Engineering stockpile. The ITC-3013 has a hemispherical beam pattern and a 12kHz resonant frequency. Following the above procedure an impedance plot was produced (Figure 3.2) and the electrical equivalent parameters were computed. From these values an initial range of 10mH - .5H of series inductance was computed to allow tuning from 5kHz to 25kHz.

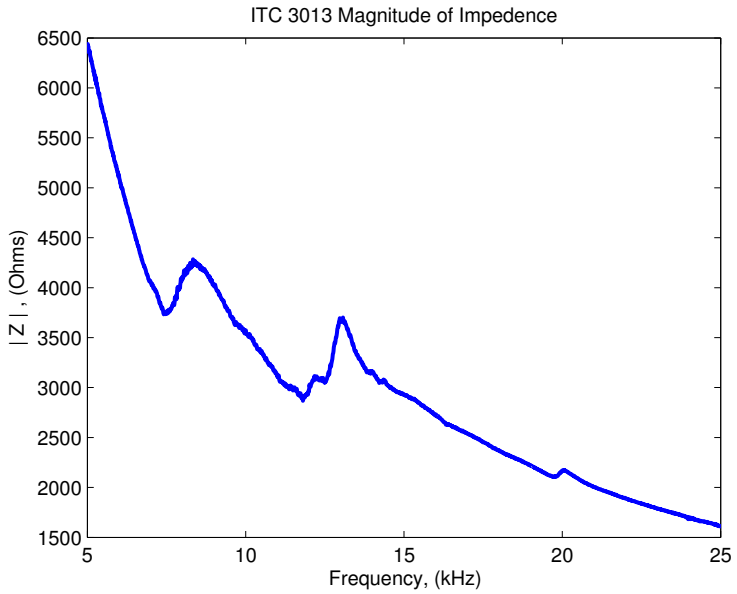

Figure 3.2: Impedance (|Z|) Curve for an ITC 3013

Finding a company to produce a custom wound multi-tap inductor for audio frequency's proved challenging. A UK based company, Sowter Transformers, was chosen and a 6 tap custom inductor was ordered. Unfortunately, the lead time for custom components from Sowter was listed as 3-6 weeks, two months later the inductor finally arrived. The Sowter 9858f is a toroidal inductor with taps fitted at 34mH, 61mH, 108mH, 145mH, 277mH, and 420mH.

The inductor was hooked up in series between the calibrated resistor and the transducer, the system was excited using a 100Hz to 40kHz Linear Frequency Modulation (LFM) chirp. Impedance measurements were made at all of the inductance taps, only the 34mH tap showed any effect on the impedance plot of the transducer, a phase shift above 20kHz. Something was wrong. Going back and revisiting the initial calculations a desired series tuning inductance of 1mH-50mH was calculated. Due to a typo or calculation error, the initial calculation was an order of magnitude off making the majority of the Sowter inductor's taps useless for the experiment. Using an LCR meter (BK 879B) the inductance values given by Sowter were verified, then the inductance was measured between all of the possible tap combinations, it turned out that the inductance between the 34mH and 61mH taps was 24mH. The experiment was repeated using the 24mH taps.

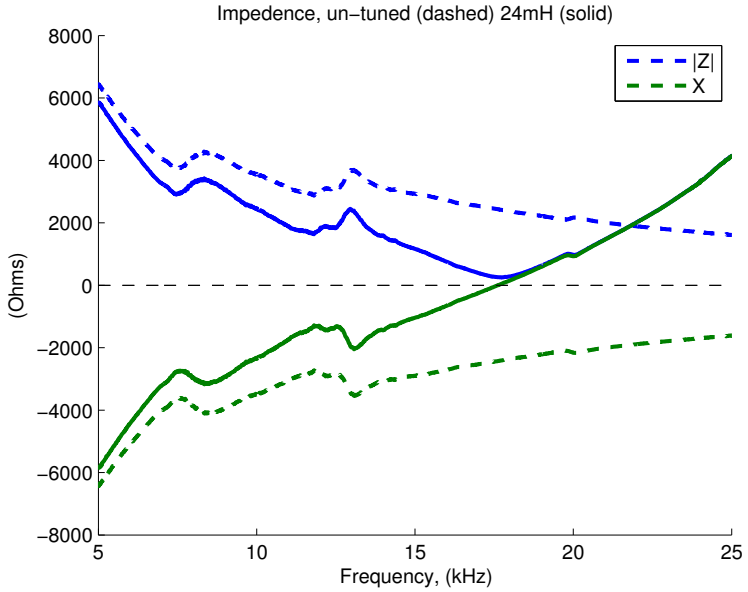

Figure 3.3: Impedance plot of the ITC 3013 with no tuning (dashed line) a 24mH series tuning inductor (solid line). The magnitude of impedance (|Z|) is in blue and the reactance (X) is in green.

Figure 3.3 shows the effect of adding the 24mH tuning inductor. The tuning inductor reduces the reactance and thus the overall impedance of the transducer

at frequencies below 22kHz. At 17.6kHz the impedance of the tuned transducer becomes purely resistive indicating that the capacitive reactance has been completely canceled. Beyond 17.6kHz the reactance becomes positive indicating that the reactive portion of the system is purely inductive. By considering the reactance of the un-tuned transducer as purely capacitive the theoretical inductance needed to cancel it out can be given by $L_s = X/\omega$ substituting the measured values $2500/(2\pi 17600) = 22.6$mH, close to the 24mH used in the experiment. The maximum test frequency of the LCR meter used in this research is 10kHz. Because of the frequency dependence of real world inductors the actual inductance of the 9858f at 17.6kHz is unknown. Potentially at 17.6kHz the inductance really is 22.6mH, but more on this in Section 3.2 .

Armed with the knowledge that the addition of a series inductor does indeed reduce the input impedance of the ITC-3013 the next logical step is to investigate the effect of tuning inductance on the transducers TVR. The ITC-3013 was suspended in the acoustics tank directly facing an ITC-1089D hydrophone located 1.2 meters away. The transducers were located centrally within the tank to limit the effects of multi-path and the data recorded was trimmed around the initial signal return. The ITC-1089D is a spherical calibrated hydrophone, it has an omni-directional beam pattern and resonant frequency of 280kHz. ITC suggests its use for signals in the .01-300kHz range and lists its sensitivity as $-216dB/1V/\mu Pa$. The ITC-3013 was excited by a 100 volt (From a Kron-Hite model 7500 amplifier) LFM chirp from .1-40kHz. Signals from the ITC-1089D were amplified using a pre-amplifier at a gain of 100x with no filtering. Measurements were taken in three configurations: 1) No tuning, the ITC-3013 is connected directly to the power amp. 2) Series tuning, the 9858f is connected between the positive signal source and one lead of the ITC-3013. 3) Parallel tuning, the 9858f is connected across the positive and negative terminals of the ITC-3013. The 24mH inductance taps of the 9858f

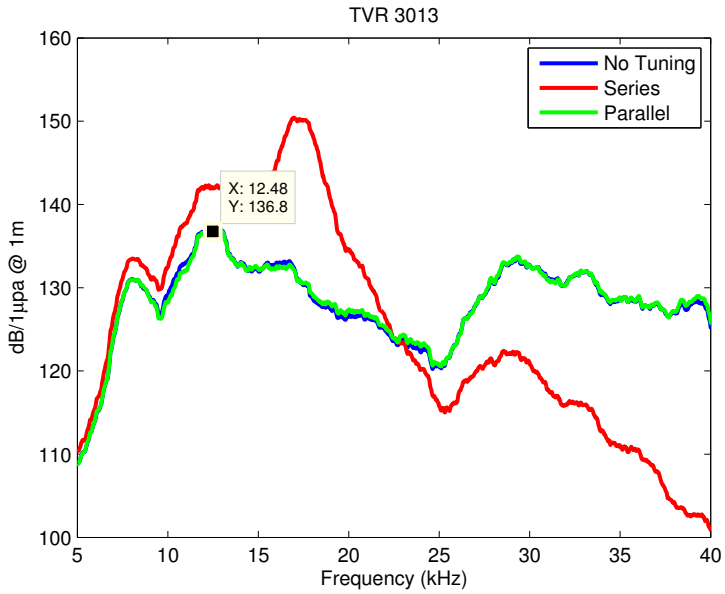

Figure 3.4: Tuned ITC-3013 TVR. The TVR is shown without tuning (blue), 24mH of series inductance (red), and 24mH of parallel inductance (green).

were used in the tuned configurations. Within MATLAB the single sided power spectral density of the received signal was computed and the resultant received voltage values were converted to the TVR using equation3.8. Finally the TVR curve was smoothed using a moving average filter.

$$\text{TVR} = 20log(V_{recieve,rms}) + \text{hydrophone sensitivity} - 20log(V_{transmit,rms}) + \text{TL} \tag{3.8}$$

By comparing the measured TVR without tuning to the TVR provided by ITC the test setup, as well as the functionality of the transducer, can be verified. According to ITC the published TVR of the ITC-3013 at resonance (12.5kHz) is $137dB/\mu Pa@1m$ the value measured in the lab was 136.8dB.

A certain amount of ambiguity existed in the literature in regards to the configuration of the tuning inductor and its effect on the TVR. [2, 3] cited that there was no benefit to the TVR of a transducer with the addition of a parallel inductor, [1, 11] claimed just the opposite. Perhaps this is because both [1] and [11] were

considering the case where a transformer doubled as a parallel inductor. Regardless Figure3.4 shows the effect of adding a 24mH inductor in parallel and in series to the transducer. The voltage response of the series tuned ITC-3013 increased below 22kHz. This comes as no surprise as this was the same band across which the impedance was reduced. At the tuned frequency (the impedance minimum), 17.6kHz, the TVR reaches its maximum of 150dB a 20dB gain over the un-tuned case. As expected, the addition of a parallel tuning inductor, had no significant effect on the TVR.

The first stage of the experiment verified that the addition of a series inductor can increase the transmitting voltage response of a transducer. Additionally, the confusion surrounding the configuration of the tuning inductor is resolved. The effects of adding a series inductor was not explored very throughly. Only one transducer was tested with a tuning inductor and only one inductance value was used, resulting in the transducer being tuned at an off resonant frequency. In order to further investigate the effects of tuning, additional inductance values would need to be tried. Replacing the Sowter 9858f with a more variable alternative became a priority.

3.2 Variable Inductors

Although computing technology has advanced significantly since Polk's work in 1978, the design and construction of large (mH-H) variable inductors and transformers remains largely unchanged. Certainly there have been remarkable advances in the form-factor and efficiency of small value inductors and transformers; however, larger inductors rated for RF frequencies seem to have been left behind. Companies such as Variac, whose main focus is large bench top variable power transformers are still producing products nearly identical to the ones they produced in 1934. Further compounding the issue, large variable inductors once

commonly used for antenna tuning in radio applications, are no longer produced in the quantities they once were, leaving the only commercial options for large variable inductors prohibitively expensive.

In an effort to obtain a variable inductor in the 1 to 50 Milli-Henry range that would operate over the frequency range of interest (5-200kHz) several different avenues were explored. The custom wound multi-tap inductor from Sowter Transformers employed in section 3.1 was useful to demonstrate viability of tuning. However the 9848f lacked the adjustment resolution desired. Additionally, the lead time of custom wound components made ordering additional Sowter components prohibitive. A hunt for discontinued General Radio RF inductors (specifically model GR-107M) involved contacting numerous surplus electronics companies and yielded tons of vintage variable inductors, yet none in the range of inductance required for the project. Wiring a Variac autotransformer as an inductor a range of .1mH-10H was measured between the wiper and one end of the coil. However, only at exceedingly low frequencies, at 100Hz the self resonant frequency of the inductor had already been reached. As the Variac is designed for AC power applications (50/60Hz) this was unfortunate but not surprising. Several attempts were made at producing a custom wound variable inductor in house. Using a plastic bobbin wrapped in 32Ga magnet wire and a moving ferrite coil several functioning variable inductors were constructed. All of these laboratory prototypes exhibited a strong frequency dependence which made them unsuitable for the project.

3.2.1 Construction

Fortunately, finding fixed inductors which exhibited the frequency characteristics of the desired system was significantly easier. 1mH inductors with self resonant frequencies in the MHz are readily available from a variety of sources. Although larger inductors are also available, simple cylindrical core inductors exhibited much

lower self resonant frequencies, and the large toroidal components were exponentially more expensive. Theoretically inductors simply add in series, so in an effort to produce an inexpensive 50mH inductor which met the frequency requirements of the project 50 1mH inductors (EPCOS B82145A1105J) were ordered from Mouser Electronics. Not only were 50 1mH inductors significantly cheaper than ordering another Sowter custom component the parts arrived in 2 days, much quicker than the typical 2 month order from Sowter. This approach would allow construction of a "variable inductor" with approximately 1mH resolution.

After verifying that inductors do indeed add in series, the inductors were arranged on a prototype board with each component mounted at 90 degree angels to its neighbor in an attempt to minimize issues with mutual inductance. Placing the components at right angles to one another is an inefficient use of board space, but placing the components parallel to one another yielded unpredictable inductance values. Six "banks" of inductance values were wired, having the values of 1mH, 1mH, 3mH, 5mH, 10mH, and 20mH. It might have made more sense to go with a binary scheme, but because of the way the inductor banks were eventually automated it would have made no difference. Even with the right angle configuration each bank had to be "adjusted" to compensate for the effects of mutual inductance, this was done by bending individual inductors farther from their neighbors.

3.2.2 Testing

Using an RLC meter the inductance of each bank of inductors was adjusted to match the design specifications. As noted previously the BK RLC meter has a maximum test frequency of 10kHz, because of this the performance of the prototype inductor network could not be verified across the entire frequency range of interest. A real world inductor can be represented by a resistor and inductor in parallel with a capacitor. As the wire has some intrinsic resistance, and the spacing between

the windings of wire generates some capacitance (There is some debate on this subject, an alternative representation of the capacitance is related to the half wave length of the signal and the length of wire used in the windings[4]. RLC meters essentially perform an impedance measurement and calculate the capacitance or inductance from the reactance, similar to the way transducers are measured in the lab. The same test setup used in the lab for transducer impedance evaluation was used to measure the frequency dependence of the prototype inductors.

Following the procedure outlined in section 3.1 for impedance measurements an inductor was substituted in place of the transducer in Figure 3.1. A Bourns 470mH RF inductor was selected to test this method as its Self Resonant Frequency (SRF) was provided by the manufacturer as 54kHz, a frequency well within the capabilities of the Lab test equipment. This test was performed on a single 470mh inductor as well as on two 470mH inductors in series. The inductance at 10kHz was first verified using the RLC meter as 470mH for the single inductor and 940mH for the two in series. The inductor was excited using a 1V .1-100kHz LFM sweep. A MATLAB script was written to plot the resistance, reactance, and magnitude of the impedance. Additionally, the inductance was calculated from the reactance. Figures 3.5 and 3.6 show the results of the single and series inductor impedance measurements.

The results of this test indicated a SRF of 10.34kHz for the single 470mH inductor and 7kHz for the series 940mH case. Obviously, these self resonant frequencies are much lower than the 54kHz provided by the product data sheet. Additionally, the inductance appears to be wildly frequency dependent and is much higher than it should be. Furthermore, the measurements didn't agree with the LCR meter, at 10kHz the computed inductance for the 470mH case was 3.3H nearly an order of magnitude off. For the 940mH case the computed reactance indicated that the series inductors were behaving capacitively. Either the manufacturer's specs were

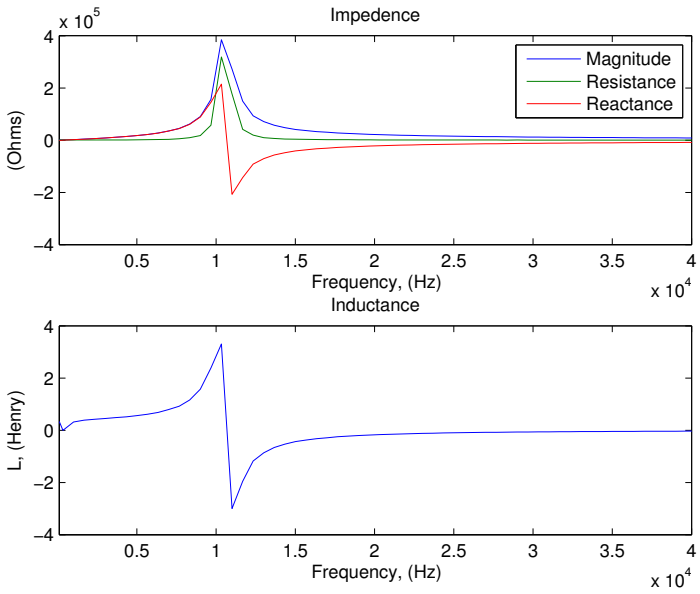

Figure 3.5: Single Bourns 470mH inductor.

in error and the LCR meter flawed or something was wrong with the test setup. Logically the later option seemed much more likely.

The test was repeated for the single 470mH inductor with a Tektronix Oscilloscope replacing the National Instruments DAQ. This time the SRF of the inductor was calculated to be 21.1kHz, closer but still off by a factor of two. More importantly one must determine why the results of these tests were different. According to the product manuals the oscilloscope and DAQ have nearly identical input electrical characteristics, a several megohm impedance and a parallel capacitance of 10pF. By reevaluating the test setup Figure 3.1 can be redrawn as the equivalent circuit in Figure 3.7 where the groups of a parallel resistor and capacitor represent the input parameters of the data acquisition device, be it the DAQ or Oscilloscope.

Its easy to take the measurements provided by test equipment at face value and forget that in order for the test equipment to actually measure the circuits they are connected to they must actually become part of that circuit. Rather than measuring the impedance of just an inductor the actual measurement is of a parallel RLC circuit where the resistive and capacitive components are contributed

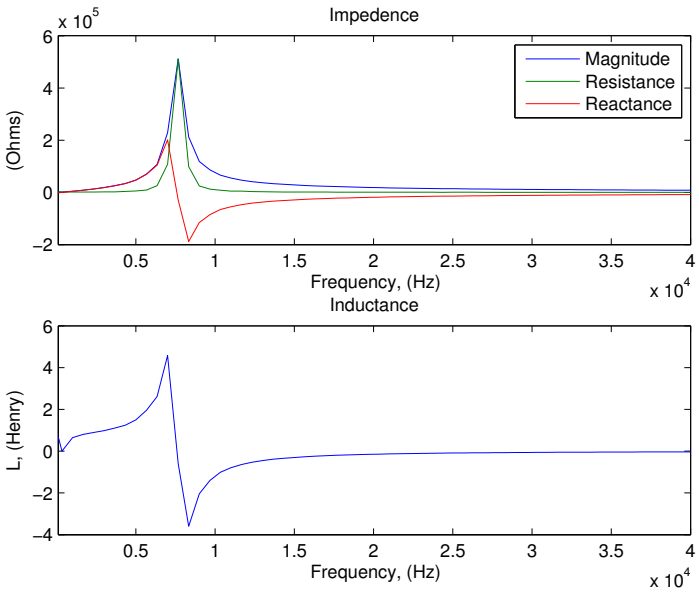

Figure 3.6: Two Bournes 470mH inductors in series.

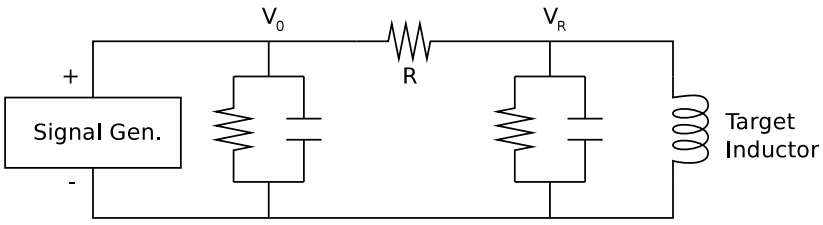

Figure 3.7: Inductor test setup equivalent circuit.

by the test equipment. Using the LCR meter the input capacitance of every part of the data acquisition system was measured. These measurements (Table 3.1) indicate not only that there is a significant amount of capacitance in the BNC test leads but also that the NI DAQ has an input capacitance significantly above that specified by the manual. After weeks of discussion with technical support at National Instruments it turned out that the input capacitance specified for the DAQ only represented the physical connector not the inner workings of the device (which one could argue is useless measurement) and that the amplifier within the DAQ has an input capacitance of 100pF. The cable and BNC 2110 (the breakout board for the DAQ connections) are also not included in the specifications. Finally the NI support staff concluded that there was nothing wrong with the DAQ but

Component(s)	Capacitance (pF)
BNC Test Lead	103
BNC Lead+Tektronix Oscope	117
BNC Lead + BNC 2110 + Cable + NI 6110 DAQ	499
BNC Lead + BNC 2110 + Cable	384
BNC Lead + BNC 2110	103

Table 3.1: Equipment Input Capacitance.

they could suggest several other NI products with lower input capacitances.

Armed with the knowledge that the input inductance of the DAQ is not trivial the equivalent circuit of the test setup (Figure 3.7) can be treated as an RLC circuit and its resonant frequency can be evaluated using $\omega = 1/\sqrt{LC}$ applying the measurements from Table 3.1 yields a resonant frequency of 21.14kHz for the oscilloscope case and 10.38kHz for the DAQ case when testing the 470mH inductor. Nearly identical to the results of the impedance test. Returning to Figures 3.5 and 3.6 it appears that significantly below resonance the calculated inductance corresponds with the values from the LCR meter and factory values. Thus the impedance measurements taken in section 3.1 with the addition of a 24mH series inductor are still valid (the resonance for that case is 46kHz, well above the region of interest). Unfortunately, it also appears that neither the DAQ nor the oscilloscope can be used to measure the self resonant frequency of a large inductor.

Typically, the underwater transducers calibrated using the NI DAQ 6110 at the URI Acoustics Tank have capacitances in the 3-15nF range so the addition of .5nF of capacitance to every transducer that an impedance measurement is made upon is somewhat troubling. Fortunately, the impedance measurements taken on the ITC-3013 are nearly identical to the factory supplied calibration curves. So for the time being it's likely safe to conclude that the effects of the added capacitance on transducer impedance measurements are negligible. Even so the remainder of the investigation into inductive tuning will rely upon TVR measurements rather

than impedance measurements.

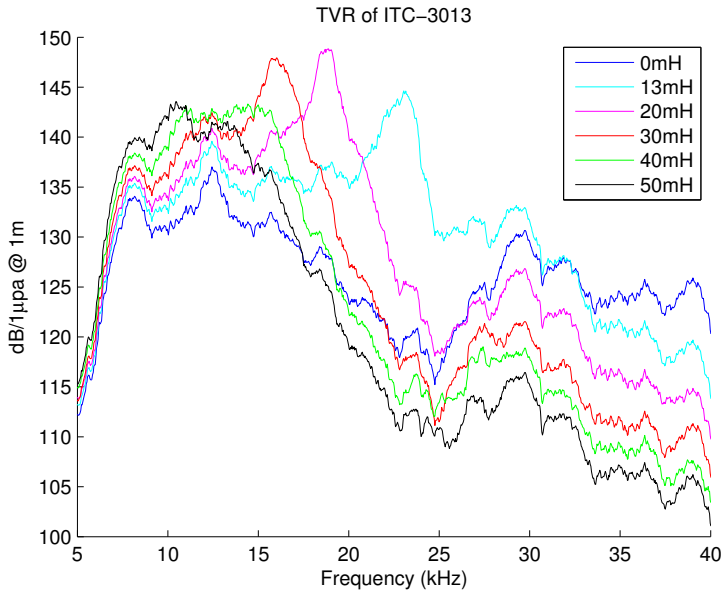

Figure 3.8: Tuned ITC-3013 TVR at multiple series inductance values.

Following the test procedure listed in 3.1 for TVR measurements the inductor banks were connected in several configurations The Results of this test are pictured in Figure 3.8. By comparison to Figure 3.4 the un-tuned (0mH) case is identical between the two experiments, and the 20mH case is very close to the 24mH case. Thus confirming solidarity between the separate tests. Furthermore, this test indicates that employing several banks of small inductors wired in series is an effective alternative to larger custom wound component. Although the actual frequency dependence of this inductor network could not be determined directly these measurements indicate that SRF of the inductor network is adequate for the requirements of this project.

3.3 Design and Construction of an Automated Tuning System

3.3.1 The Switching Inductor Network

3.1 Demonstrated that inductive tuning has the potential to increase the radiated acoustic power from a transducer. 3.2 outlined the methodology to produce a large variable inductor from a series circuit of smaller inductance values. Combining these efforts a prototype Switching Inductor Network (SIN) was built using low power mechanical relays. Each of the inductor banks outlined in 3.2.1 was connected according to Figure 3.9. This might be thought of as a somewhat unorthodox method of connecting the different banks of inductors but the design was formulated to minimize the number of IO lines required to switch between inductance values. The NI DAQ 6110 has 8 digital IO lines and this design allows for the selection 1-40mH inductance while retaining two IO lines for future expansion. The prototype Switching Inductor Network (SIN) is pictured in Figure 3.10.

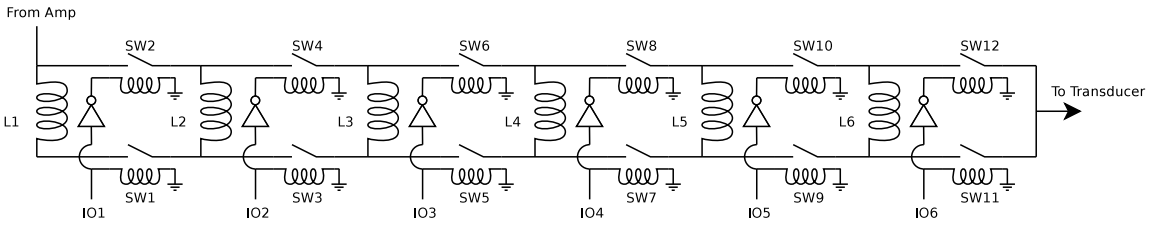

Figure 3.9: SIN Schematic

Initially the plan was to use solid state relays due to their low power consumption, however each solid state relay added 10pF of capacitance to the system. The mechanical relays (Fujitsu FTR-F3AA005E) consume significantly more power than the solid state relays sourced for the project (Panasonic AQH1213) putting them just at the limit of current that can be supplied from the inverter (NXP 74ABT04N). The prototype board incorporates a logic high/low (5v/Gnd) bus allowing SIN to be used without connection to a DAQ. The multiple inductance experiment performed in 3.2.2 was repeated using the SIN prototype to produce

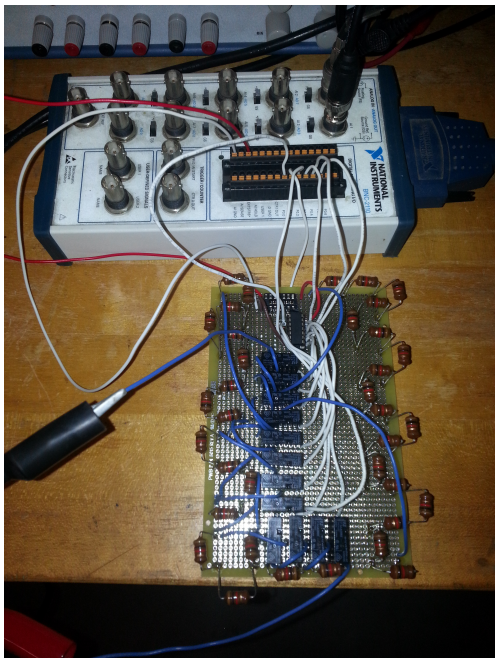

Figure 3.10: Prototype switching inductor network(SIN).

the TVR plots pictured in Figures 3.11 and 3.12. SIN was connected to the DAQ and controlled using a MATLAB script. In an effort to illustrate the effect of small value (1-5mH) series inductance on the TVR the excitation frequency range was extended to 1-75kHz.

3.3.2 The Automated Tuning System

The Automated Tuning System (ATS) is an extension of SIN which seeks to reap the benefits of inductive tuning without any operator input. The concept is relatively straightforward the desired waveform is created within MATLAB and programed to the signal generator a tuning algorithm then determines the optimum SIN settings and the signal is sent from the signal generator through an amplifier and SIN to the transducer. Optionally a feedback loop can be incorporated using a hydrophone or impedance data.

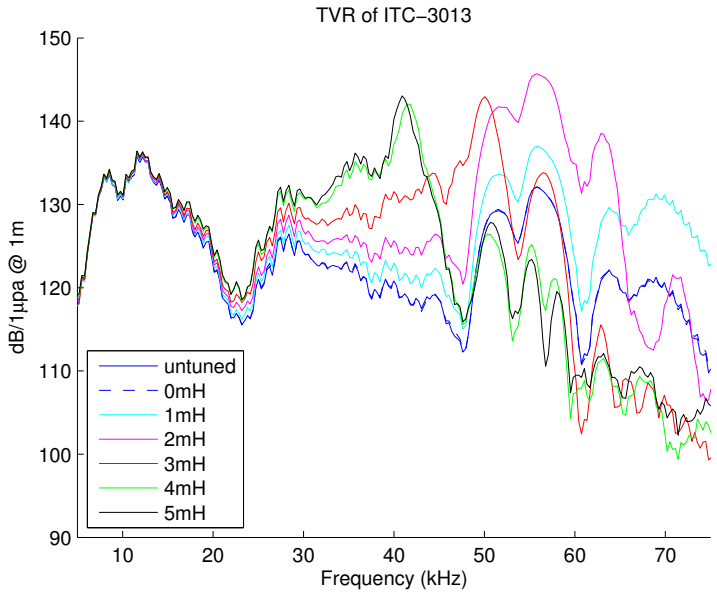

Figure 3.11: TVR of ITC-3013 connected to SIN from 0-5mH.

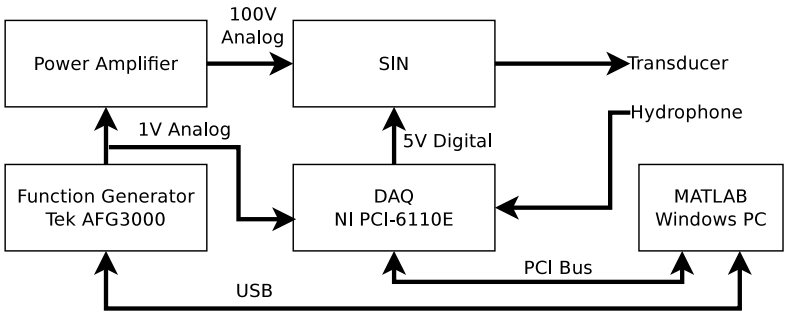

Figure 3.13: ATS Flow Chart

Figure 3.13 illustrates the connections within the ATS system: A MATLAB program running on a windows PC controls the ATS and logs the acoustic data. SIN is controlled by the DIO (Digital Input/Output) pins on the DAQ, the DIO pins can be latched high or low (+5V & 0V) to control the relays within SIN, the DAQ also supplies 5V to the logic inverter. A USB interface connects the function generator to the PC allowing the ATS algorithm to control the output waveform parameters. The analog waveform from the function generator serves as the trigger for data acquisition and is amplified 100x before being fed into the switching inductor network and fed to the transducer. A reference hydrophone

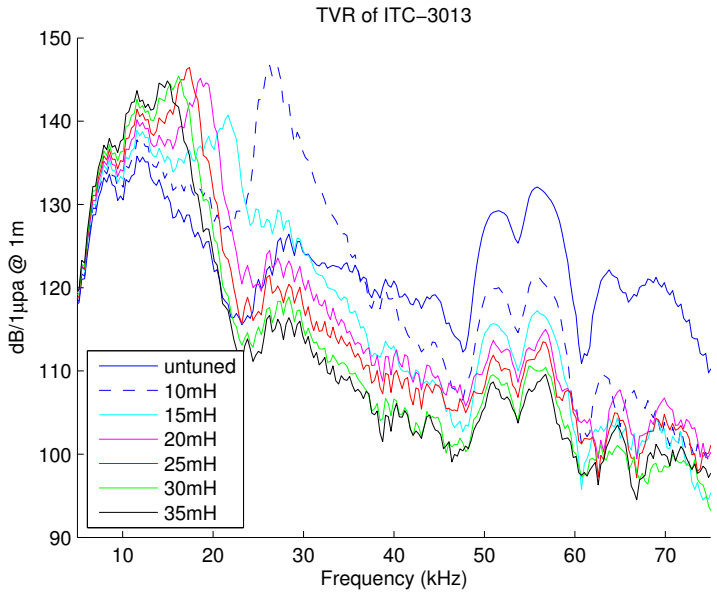

Figure 3.12: TVR of ITC-3013 connected to SIN from 10-35mH.

provides feedback data to the ATS to determine the effectiveness of the tuning parameters.

3.3.3 ATS Algorithm

The current ATS algorithm (Appendix A) implements a brute force tuning strategy, in other words it iteratively tries every inductance value. The "best" inductance value chosen to be the one which maximizes the TVR across the input frequency range. The code is limited to two different acoustic signals, an LFM chirp and a continuous wave (CW) burst. For each inductance value the TVR is windowed across the excitation signal's frequency range. The mean and standard deviation are then taken of the windowed data. The effectiveness of each inductance value is evaluated using the mean and standard deviation . The algorithm simply chooses the maximum mean as the best tuning scenario, if the corresponding standard deviation is also the maximum the algorithm notifies the user. Depending on the desired outcome of tuning the user might seek to tune the transducer to minimize the TVR deviation across the signal range. Finally, SIN

is reset to the best inductance value and the tuned TVR is plotted against the untuned TVR.

As the algorithm runs it continually updates a waveform and TVR plot. Figure 3.14 shows the output of the ATS as it iteratively tunes an ITC-3013 to a 25-27kHz LFM chirp. The TVR from the most recent dataset is plotted in red while past datasets remain plotted in black. The transmitted and received (blue and green respectively) waveforms from which the current TVR is derived are plotted to allow the user to monitor the signal for clipping and other possible behavioral issues. Figures 3.14a -3.14d clearly show the output of the transducer increasing as the ATS iteratively adds inductance. The ideal tuning inductance, as determined by the ATS, is shown in Figure3.14e. Visual inspection of the ATS output confirms that the next iteration of the system (Figure 3.14f) decreases the output of the transducer significantly. This continuous graphical output allows the user to easily visualize the effect of tunning as well as the process employed by the algorithm to determine the optimal parameters. In this case it appears that the ATS correctly determined the tuning value which maximizes the output power of the the transducer.

Creating the excitation waveform within MATLAB minimizes the signal processing performed by the ATS algorithm. The input waveform is already recorded by the system, it would be very straightforward to automatically determine the frequency content of the input waveform and extend the algorithm to perform tuning on an externally created waveform.

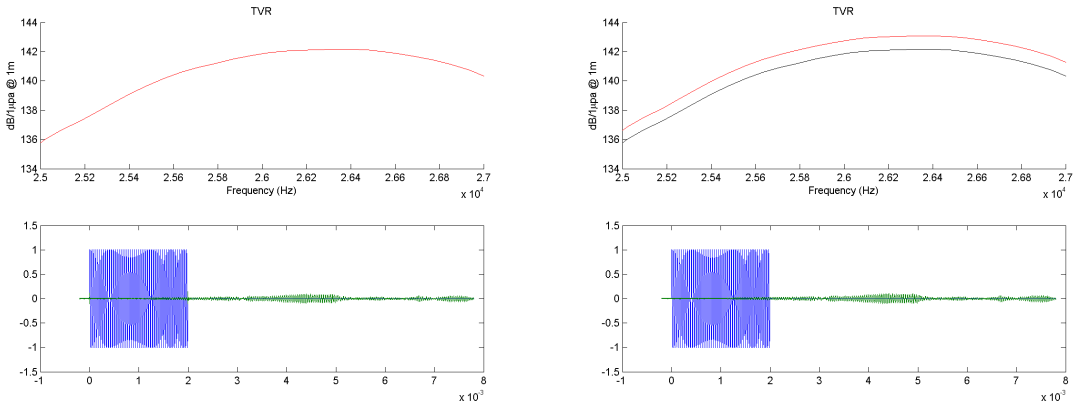

(a) 0mH

(b) 1mH

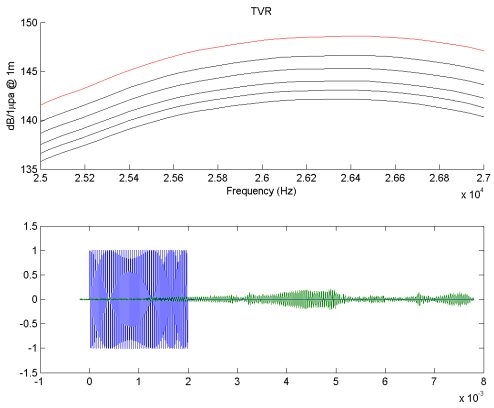

(c) 5mH

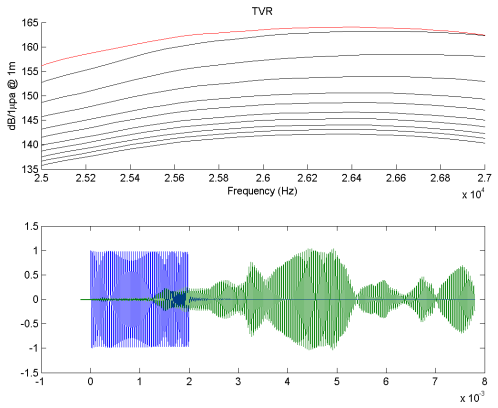

(d) 10mH

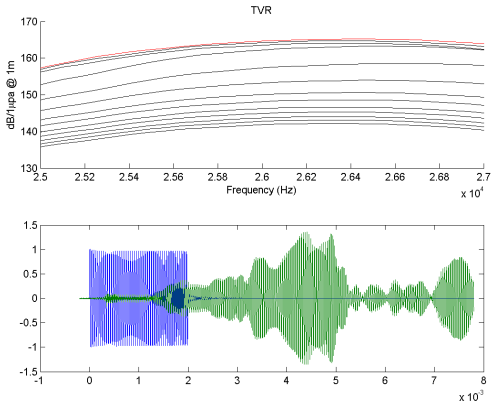

(e) 12mH

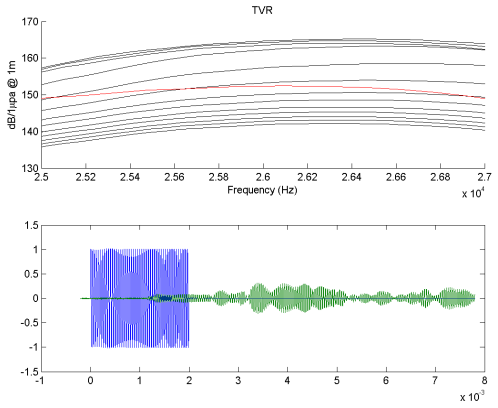

(f) 13mH

Figure 3.14: Output from running ATS algorithm (ITC-3013 25-27khz LFM chirp). In the TVR plot (top) the red line indicates the current TVR while the black lines represent the TVR from previous inductance values. In the waveform plot (bottom) blue is the transducer excitation signal while green is the signal received by the reference hydrophone (ITC-1089).

The algorithm outlined above is extremely simple and is only meant to showcase the physical functionality of the ATS. Because the program is written in MATLAB future users should be able to easily leverage MATLAB's extensive signal possessing capabilities to develop a more robust system. Furthermore the capabilities of SIN could easily be expanded, by choosing a bank of inductances whose values correspond to a binary scheme a greater range of inductive values could be used. Additionally a switching multi-tap transformer could be developed and added to the system, further increasing the output power of the system.

CHAPTER 4

RESULTS AND DISCUSSION

The effectiveness of the ATS can be quantified by: 1) Comparing the TVR plots of the transmitted signal in both the tuned and untuned configurations. 2) Examining the differences in the received Waveform in both configurations. 3) Comparing the impedance plots of both Configurations. This section includes the results of using the ATS with a variety of input waveforms and two different transducers.

Universally the ATS was able to increase the transmit response of the transducer. The ATS is capable of producing remarkable efficiency gains at off resonant frequencies, Unfortunately, these gains come at the cost of bandwidth. In general an increase in required tuning inductance yields a decrease in bandwidth. This is illustrated by the TVR plots in 4.1.2 and 4.1.3, in both cases the system produced an average gain across the input frequency band, however in both power tuned cases showed a significant peak surrounding the tuned resonant frequency.

For an input bandwidth of less than 10kHz the ATS performed flawlessly.

4.1 ITC-3013

The ITC-3013 is the transducer that has been used for all of the developmental testing outlined in the methods section, as such some of the results may seem repetitive. Bear in mind that the optimal tuning value for each of these tests was obtained automatically by the ATS.

4.1.1 Test 1

The ITC-3013 was excited with a 25-27kHz LFM chirp two milliseconds long. The ATS identified the ideal tuning inductance to be 12mH. The mean of the TVR across the test frequency was 163.3 dB with a standard deviation of 2.2 dB. From the TVR plot (Figure 4.1a) its evident that the ATS increased the transmitted response of the transducer nearly uniformly across the band. Furthermore the tuned impedance plot (Figure 4.1b) shows that the impedance of the transducer not only becomes purely resistive at the chirp center-frequency (26kHz) but also becomes near zero a significant reduction from the untuned case.

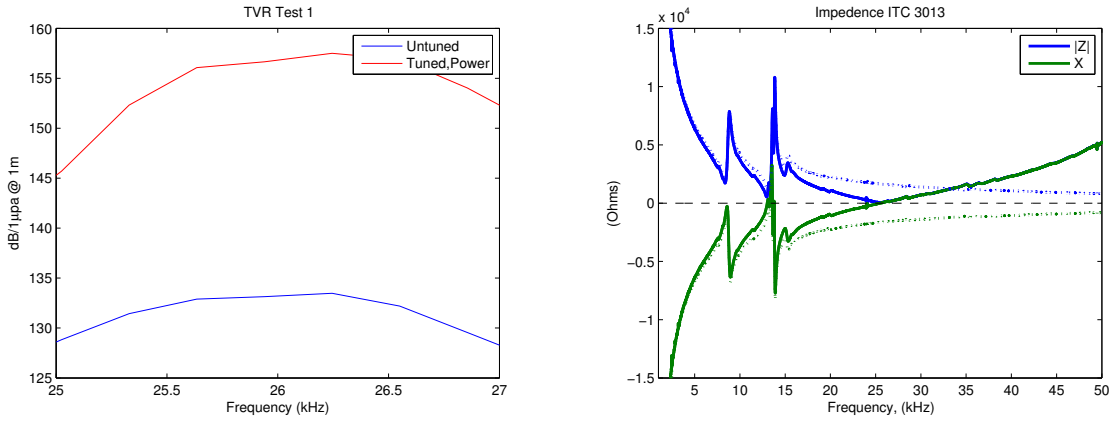

(a) (b)

Figure 4.1: ITC-3013 Test 1 TVR (a) & Impedance (b, Dotted = Untuned, Solid = Tuned).

Both the tuned and untuned waveforms (Appendix 1) show a decrease in amplitude near the 3ms mark indicating that the addition of tuning inductance may not have decreased the Q of the system to an unusable value. However, due to the long chirp length (relative to the size of the acoustics tank) there is a strong multi-path return in both the tuned and untuned transducers nearly immediately after the initial signal, making a visual estimate of transducer ringing impossible.

4.1.2 Test 2

The 3013 was excited with a 5-30kHz LFM chirp two milliseconds long. The ATS identified the ideal tuning inductance to be 13mH. The mean of the TVR across the test frequency was 142.6 dB with a standard deviation of 7.5 dB. Because of the strong roll off in efficiency beyond the tuned resonance it appears that the ATS chose a tuning value which placed the impedance minimum (25kHz, see Figure 4.2b) near the maximum chirp frequency. The TVR plot (Figure 4.2a) shows an increase in the transmitted response across the majority of of the chirp bandwidth, below 7kHz the gains are negligible. The gains are significantly more pronounced near the tuned resonance, this resonance produced a peak approximately 10dB above the rest of the tuned frequency range with a bandwidth of 7kHz.

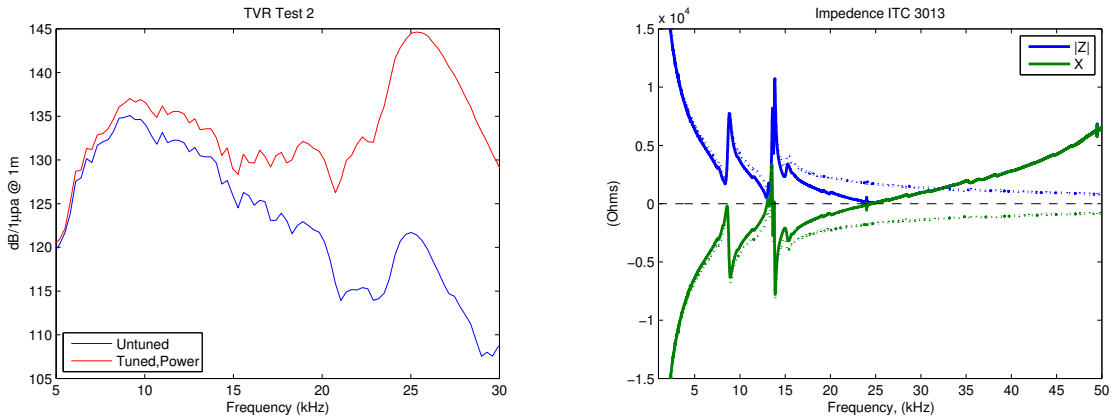

(a) (b)

Figure 4.2: ITC-3013 Test 2 TVR (a) & Impedance (b, Dotted = Untuned, Solid = Tuned).

4.1.3 Test 3

The 3013 was excited with a 5-50kHz LFM chirp two milliseconds long. The ATS identified the ideal tuning inductance to be 8mH. The mean of the TVR across the test frequency was 134.8 dB with a standard deviation of 10.6 dB. Although tuning results in gains across the majority of the spectrum, past the tuned resonance

(30khz) the response decreased. The ATS tuning resulted in a 15dB peak around the tuned resonance with a bandwidth of 10kHz. Although this would be desirable for a signal in this region the characteristics of the tuned system across the input bandwidth are rather poor.

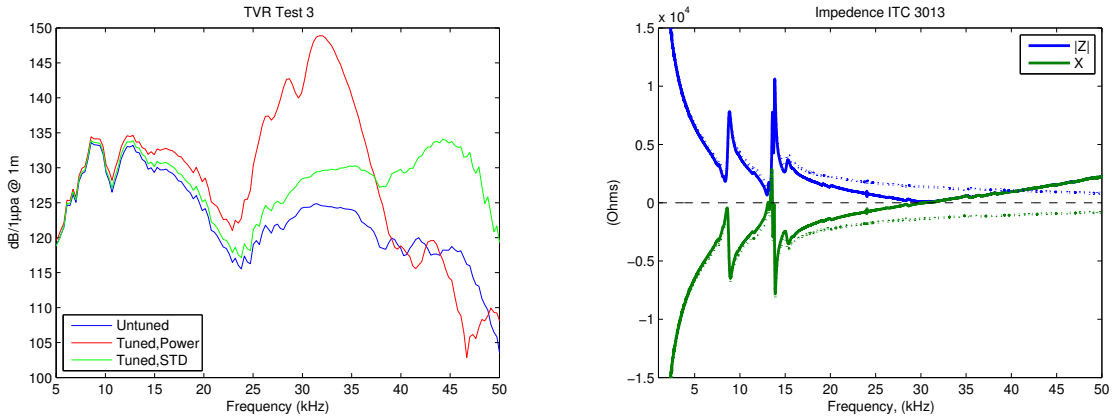

(a) (b)

Figure 4.3: ITC-3013 Test 3 TVR (a) & Impedance (b, Dotted = Untuned, Solid = Tuned).

In this case it may have been more effective to attempt to tune the system to minimize the deviation rather than maximize mean output power. Figure 4.3a shows a comparison of the untuned (blue), ATS tuning for power (red), and ATS tuning for deviation (green). The TVR exhibited the following characteristics: untuned mean 128.6dB deviation 5.5dB, tuned for power mean 134.9dB deviation 10.6dB, tuned for deviation mean 134.5dB deviation 4.9dB. With the ATS set to tune to minimize deviation the mean output power decreased by less than one decibel yet the deviation decreased below the untuned value to less than half of the tuned deviation. In this case the bandwidth of the ITC-3013 has effectively been doubled. Additionally the TVR increased across the entire frequency band rather unlike in the power tuned case. In this case tuning to minimize the deviation offered the ideal tuning value. Further development of the ATS algorithm should make this decision automatically.

4.1.4 Test 4

The 3013 was excited with an 18 kHz CW burst two milliseconds long. The ATS identified the ideal tuning inductance to be 22mH. The mean of the TVR across the test frequency was 152.7 dB with a standard deviation of 9.7 dB. At the tuned frequency the ITC 3013 exhibited a gain of 20dB over the untuned case. The impedance plot (Figure 4.4b) shows that the ATS tuned the transducer to be almost purely resistive near 18kHz reducing the magnitude of impedance from $2.5k\Omega$ to $0.15k\Omega$.

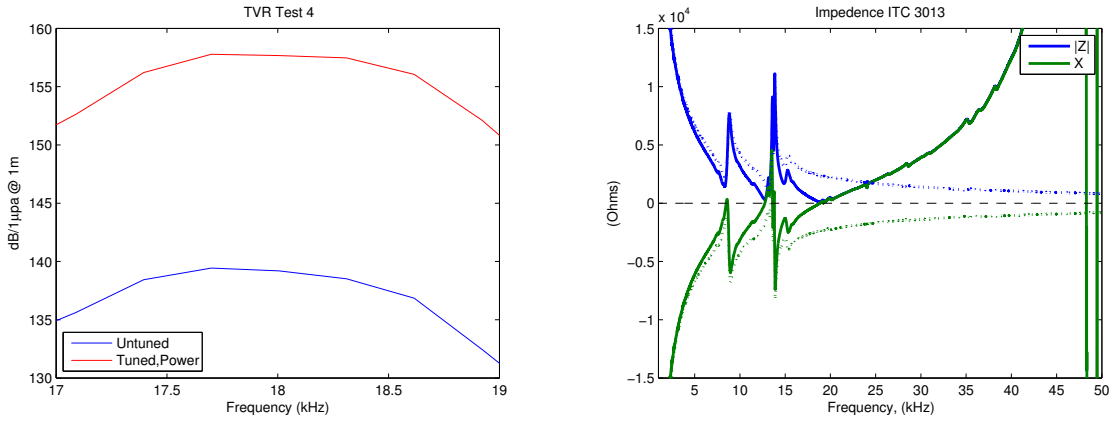

(a) (b)

Figure 4.4: ITC-3013 Test 4 TVR (a) & Impedance (b, Dotted = Untuned, Solid = Tuned).

4.2 Prototype Transducer

As the goal of this project is to produce a method to automatically tune a transducer with no prior knowledge of its parameters it seemed prudent to test the ATS with an unknown transducer. Another ongoing project at the university aims to produce very low-cost high-power transducers, while the ITC-3013 costs several thousand dollars the cost of this prototype transducer is less than a hundred dollars. This low cost transducer is constructed of salvaged cable and a Tonpilz resonator epoxied within a PVC housing. A photograph of the prototype trans-

ducer can be seen in Figure 4.5. An impedance plot (derived following 3.1) can be seen in Appendix 4, where it appears that the prototype transducer has a resonant frequency near 30kHz.

Figure 4.5: The prototype transducer.

4.2.1 Test 1

The prototype transducer was excited with a 15-20kHz LFM chirp .8 milliseconds long. The ATS identified the ideal tuning inductance to be 6mH. The mean of the TVR across the test frequency was 156.8 dB with a standard deviation of 2.2 dB. Again we see that the ATS minimizes the impedance at the center frequency of the chirp.

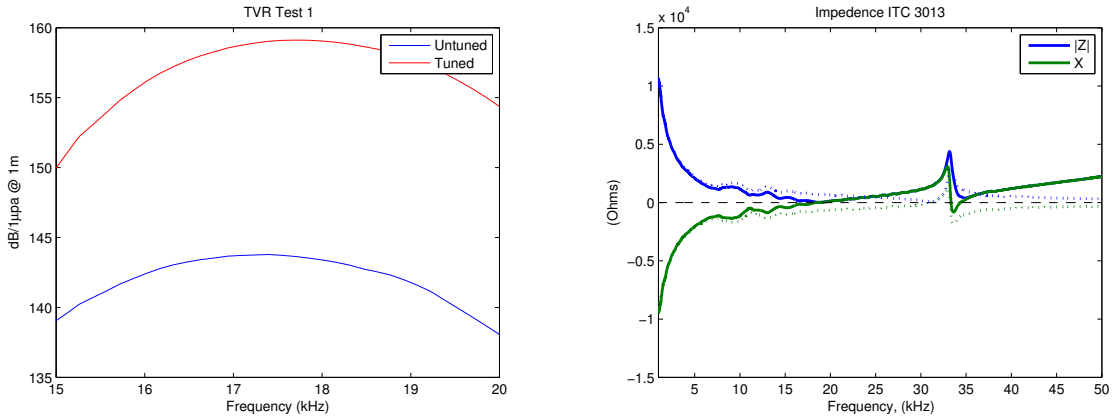

(a) (b)

Figure 4.6: Prototype transducer Test 1 TVR (a) & Impedance (b, Dotted = Untuned, Solid = Tuned).

4.2.2 Test 2

The prototype transducer was excited with an 10 kHz CW burst 5 cycles (.5ms) long. The ATS identified the ideal tuning inductance to be 20mH. The increase in response at the tuned frequency was 15dB. The comparison of waveforms in Figure 4.8 shows a negligible difference in ringing between the tuned and untuned cases.

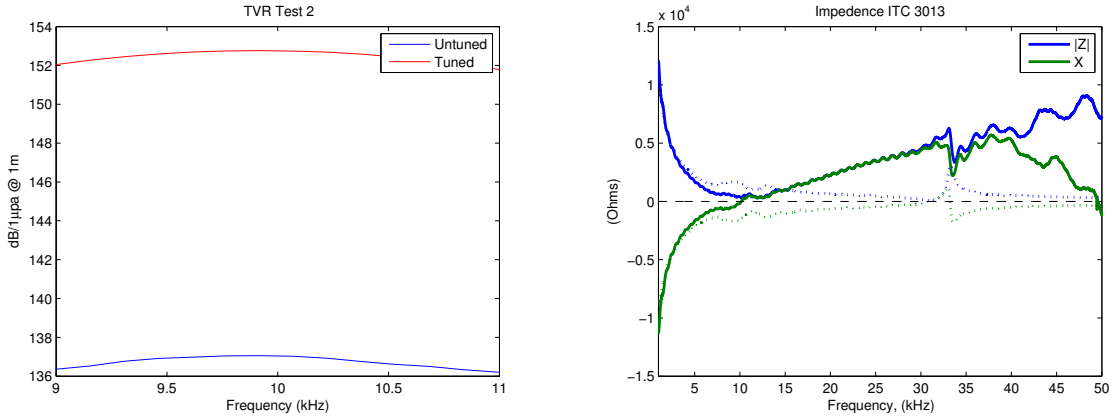

(a) (b)

Figure 4.7: Prototype transducer Test 2 TVR (a) & Impedance (b, Dotted = Untuned, Solid = Tuned).

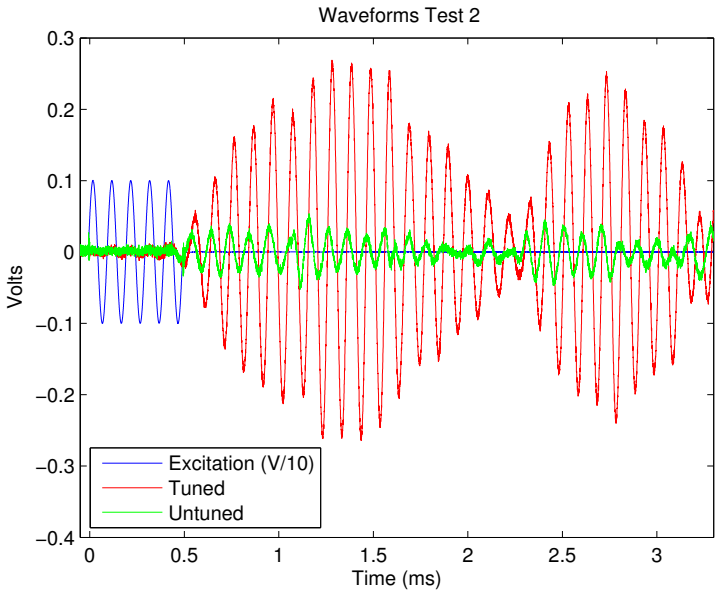

Figure 4.8: Prototype transducer Test 2 Waveforms.

CHAPTER 5

CONCLUSION

The aim of this project was to design and test a system which automatically tuned a transducer within a laboratory setting. The result of this effort is the Automated Tuning System. Testing confirms that the ATS effectively increases the transmit response of a transducer under a variety of conditions. In some cases the ATS was capable of increasing the TVR in excess of 15dB, in other cases the ATS was able to double the functional bandwidth of a transducer. Universally, the ATS arrived at a result which increased the TVR of the target transducer, thus the primary aim of the project was a success.

The development of the ATS offered a detailed investigation into the methods and equipment typically employed for transducer evaluation. Furthermore potential issues related to the electrical characteristics of the test equipment were discovered. An intuitive method for producing large variable inductors was developed and successfully tested. The Switching Inductor Network functioned reliably over hundreds of hours of use, the variation in each inductance setting deviated less than a percent over the course of testing.

So far the prototype ATS is only a proof of concept, there are plethora of directions in which future development could proceed. SIN could easily be extended to provide a greater range of inductances. The switching concept of SIN could be applied include additional components (transformers, capacitors, etc), in various configurations, into the tuning network. More advanced tuning networks

such as the T network could be constructed with switched components. The existing ATS prototype could also be tested to improve the receive characteristics of hydrophones.

Appendix

A) ATS Algorithm:

```
function [meanTVR, TVRstd, TVdata, Lbest] = ...

     ATS( Fstart, Fstop, PulseLength, L )

%ATS Drives the Automated Tuning System (ATS).
warning off all;
addr = 'june19/sewer/test4/';
fend = 'mH.eps'; fendj = 'mH.png'; fendmat = 'mH.mat';
load('Lval.mat'); %load the inductor lookup table
%Send signal to Function Generator
TekChirp(Fstart,Fstop, PulseLength,1,1);
% Initialize NI DIO lines
dio = digitalio('nidaq', 1);
addline(dio, 0:5, 0, 'Out');
putvalue(dio, [0 0 0 0 0 0]);
if Fstart == Fstop

     Fstart = Fstart - 2e3;
     Fstop = Fstop + 2e3; end

if isempty(L)

      figure;
     [meanTVRUN, TVRstdUN, TVRrangeUN,Data,t] = ...
         atsTVR(Fstart,Fstop,PulseLength);
     for i = 1:1:39
         putvalue(dio, Lval(i,:));
         pause(2); %
         saveas(gcf, [addr num2str(i-1) fend], 'eps') %
         saveas(gcf, [addr num2str(i-1) fendj], 'png') %
         save([addr num2str(i-1) fendmat],'Data','t');
         [meanTVR(i), TVRstd(i), TVdata(i,:),Data,t] = ...
             atsTVR(Fstart,Fstop,PulseLength);
```

```
        disp(i)
    end %
    saveas(gcf, [addr num2str(i) fend], 'eps') %
    saveas(gcf, [addr num2str(i) fendj], 'png') %
    save([addr num2str(i) fendmat],'Data','t');
    Lbest = find(meanTVR == max(meanTVR));
    disp('Maximum power output using an inductance of ');
    disp(Lbest);
    disp('mH');
    disp('mean: ');
    disp(meanTVR(Lbest));
    disp('  standard deviation: ');
    disp(TVRstd(Lbest));
    putvalue(dio, Lval(Lbest,:));
    pause(2)
    figure;
    plot(TVRrangeUN,'-b')
    hold on
    plot(TVdata(Lbest,:),'-r')
    hold off

else

    putvalue(dio, Lval(L,:));
    [meanTVR, TVRstd, TVdata] = atsTVR(Fstart,Fstop,PulseLength);
    Lbest= []; end

delete (dio);
clear dio;
end
function [ mTVR, stdTVR, target ,Data,t] = ...

    atsTVR( Fstart, Fstop, PulseLength)

%atsTVR Summary of this function goes here
Fs=5e6;
```

```
[Data,t]=nidaqmgl(1,[0 1],[2 1],...
     'Software',Fs,.002+PulseLength*3,1,.5,1000);
NFFT = 2^nextpow2(length(Data(:,2)));
Y = fft(Data(:,2)/100*.707,NFFT)/length(Data(:,2));
f = Fs/2*linspace(0,1,NFFT/2+1);
TVR = abs(20*log10(sgolayfilt(2*abs(Y(1:NFFT/2+1)), ...
     3,55))+216+20*log(1.7));
target = TVR(find( (f > Fstart) & (f < Fstop)));
mTVR = mean(target);
stdTVR = std(target);
% Plot TVR and Waveform.
subplot(2,1,1);
hold on
set(findobj('Type','line'),'Color','k');
plot(f,TVR,'-r');xlim([Fstart,Fstop]);
hold off
title('TVR')
xlabel('Frequency (Hz)')
ylabel('dB/1\mupa @ 1m')
subplot(2,1,2)
plot(t,Data);
end
```

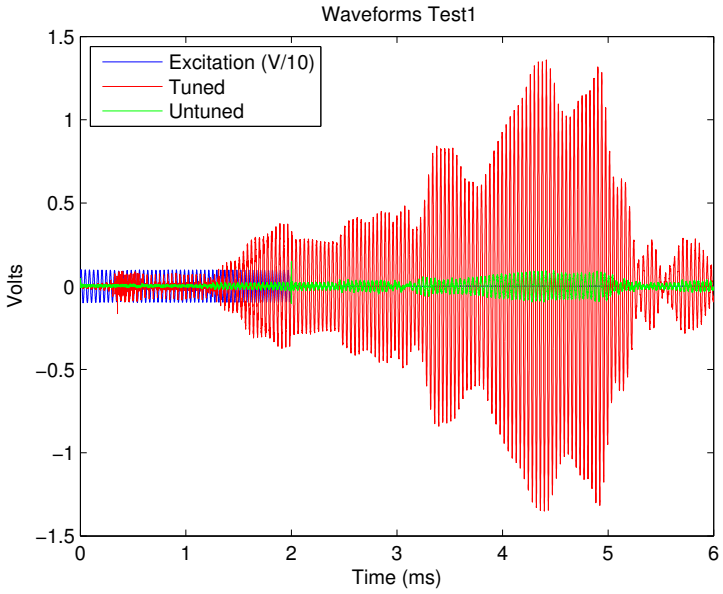

Figure 1: ITC-3013 Test 1 Waveforms.

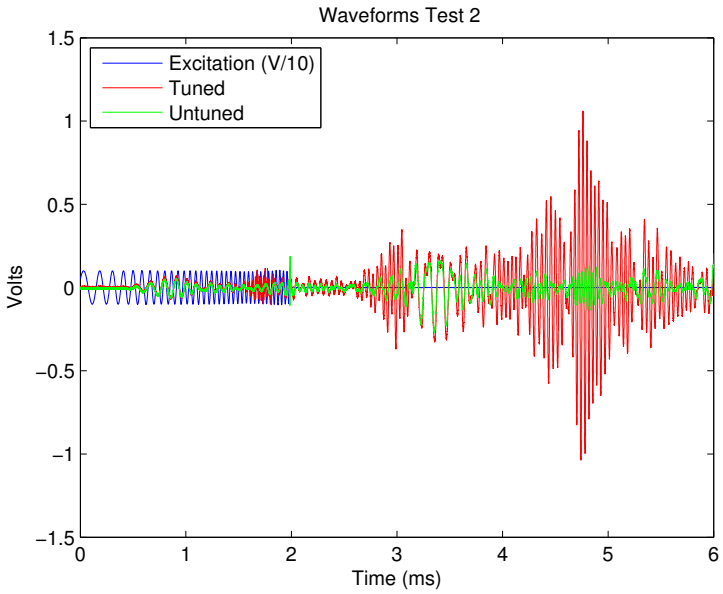

Figure 2: ITC-3013 Test 2 Waveforms.

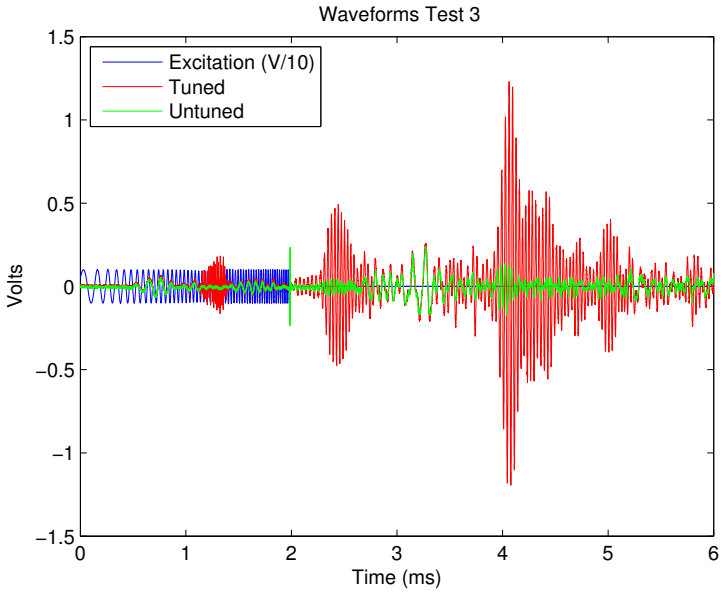

Figure 3: ITC-3013 Test 3 Waveforms.

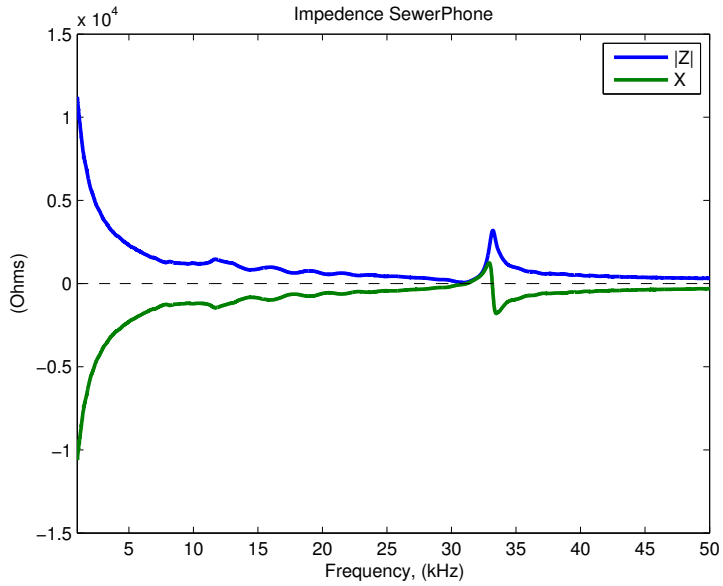

Figure 4: Prototype transducer Impedance plot.

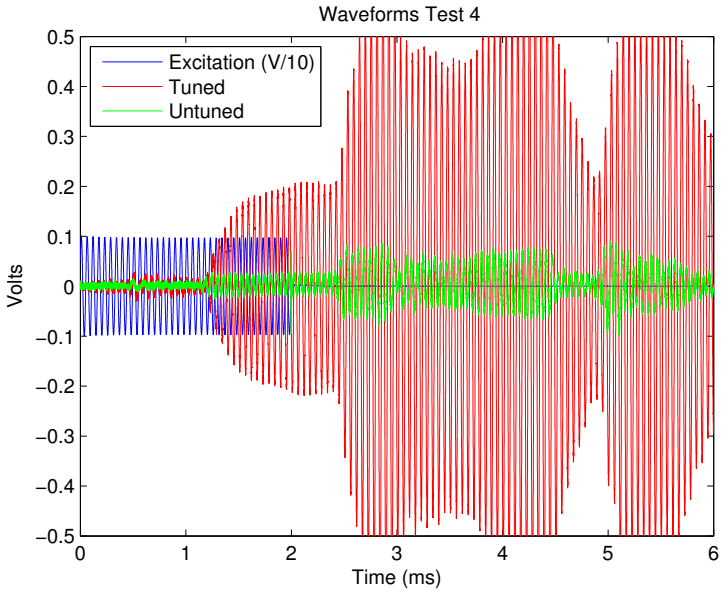

Figure 5: ITC-3013 Test 4 Waveforms.

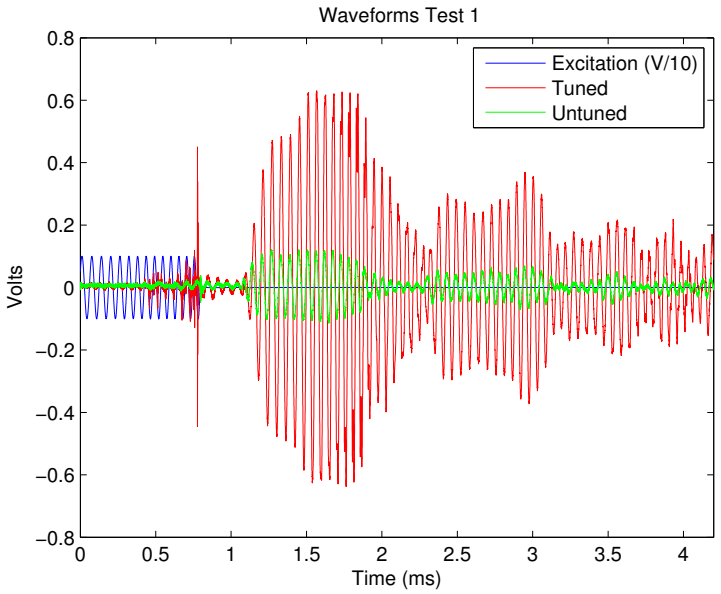

Figure 6: Prototype transducer Test 1 Waveforms.

BIBLIOGRAPHY

[1] AIRMAR Technology Corporation. "Sensor Design Fundamentals." http://www.marinop.it/pdf_doc/Transducer%20Design.pdf (June 25, 2013).

[2] Arnau, Antonio. "Piezoelectric Transducers and Applications." Springer, NY, 2010.

[3] Butler, J L. "Transducers and Arrays for Underwater Sound." Springer, NY, 2007.

[4] Clifton Laboratories. "Self Resonant Frequency of an Inductor." http://www.cliftonlaboratories.com/self-resonant_frequency_of_inductors.htm (June 2013).

[5] Fleming, Andrew. "Optimization and Implementation of Multimode Piezoelectric Shunt Damping Systems " IEEE/ASME Transactions on Mechatronics, vol.7, no.1, March 2002.

[6] Huang, Haiying. "Broadband Electrical Impedance Matching for Piezoelectric Ultrasound Transducers." IEEE Transactions on Ultrasonics, vol. 58, no. 12, December 2011.

[7] Polk, Eliot. "Impedance Matching Circuit for Ultrasonic Transducers." Thesis, MIT, September 1978.

[8] Ramesh, R. "Characteristics of Broadband Underwater Transducers Integrated with Tuning Coils and Cables." Proceedings of SYMPOL, 2009.

[9] Ramos, Antonio. "Improvement in Transient Piezoelectric Responses of NDE Transceivers Using Selective Damping and tuning Networks ." IEEE Transactions on Ultrasonics, vol. 47, no. 4, July 2000.

[10] Snook, Kevin. "Design, Fabrication, and Evaluation of High Frequency, Single-Element Transducers Incorporating Different Materials ." IEEE Transactions on Ultrasonics, vol. 49, no. 2,Feb 2002.

[11] Stansfield, D. "Underwater Electroacoustic Transducers." Bath University Press, 1991.

[12] Xu, Hui. "Active tuning of High Frequency Resonators and Filters." IEEE Transactions on Applied Superconductivity, vol. 11, no. 1, March 2001.